Chapter 2

Atomic structure and spectra

2.1 Atomic structure

2.1.1 The hydrogen atom and one-electron atoms

The Hamiltonian for one-electron atoms such as H, He^+, Li^{2+}, ..., can be written as

$$\hat{H} = \frac{\hat{p}^2}{2m_e} - \frac{Ze^2}{4\pi\varepsilon_0 r}, \tag{2.1}$$

where $\hat{p}$ is the momentum operator, m_e is the electron mass ($m_e = 9.10938291(40) \times 10^{-31}$ kg), Z is the atomic number (or proton number), e is the elementary charge ($e = 1.602176565(35) \times 10^{-19}$ C) and r is the distance between the electron and the nucleus. The associated Schrödinger equation can be solved analytically, as demonstrated in most quantum mechanics textbooks. The eigenvalues $E_{n\ell m_\ell}$ and eigenfunctions $\Psi_{n\ell m_\ell}$ are then described by Equations (2.2) and (2.3), respectively

$$E_{n\ell m_\ell} = -hcZ^2 R_M / n^2 \tag{2.2}$$

$$\Psi_{n\ell m_\ell}(r, \theta, \varphi) = R_{n\ell}(r) Y_{\ell m_\ell}(\theta, \varphi). \tag{2.3}$$

In Equation (2.2), R_M is the mass-corrected Rydberg constant for a nucleus of mass M

$$R_M = \frac{\mu}{m_e} R_\infty, \tag{2.4}$$

where $R_\infty = m_e e^4/(8h^3\varepsilon_0^2 c) = 10973731.568539(55)\,\mathrm{m}^{-1}$ represents the Rydberg constant for a hypothetical infinitely heavy nucleus and $\mu = m_e M/(m_e + M)$ is the reduced mass of the electron-nucleus system. The principal quantum number n can take integer values from 1 to ∞, the orbital angular momentum quantum number ℓ integer values from 0 to

$n-1$, and the magnetic quantum number m_ℓ integer values from $-\ell$ to ℓ. In Equation (2.3), r, θ,and φ are the polar coordinates. $R_{n\ell}(r)$ and $Y_{\ell m_\ell}(\theta,\varphi)$ are radial wave functions and spherical harmonics, respectively. Table 2.1 lists the possible sets of quantum numbers for the first values of n, the corresponding expressions for $R_{n\ell}(r)$ and $Y_{\ell m_\ell}(\theta,\varphi)$, and the symmetry designation $n\ell m_\ell$ of the orbitals.

n	ℓ	m_ℓ	$R_{n\ell}(r)$	$Y_{\ell m_\ell}(\theta,\varphi)$	orbital designation
1	0	0	$2\left(\frac{Z}{a}\right)^{3/2}\mathrm{e}^{-\rho/2}$	$\sqrt{\frac{1}{4\pi}}$	1s
2	0	0	$2^{-3/2}\left(\frac{Z}{a}\right)^{3/2}\mathrm{e}^{-\rho/2}(2-\rho)$	$\sqrt{\frac{1}{4\pi}}$	2s
2	1	0	$\frac{1}{2\sqrt{6}}\left(\frac{Z}{a}\right)^{3/2}\rho\mathrm{e}^{-\rho/2}$	$\sqrt{\frac{3}{4\pi}}\cos\theta$	$2\mathrm{p}_0$ (or $2\mathrm{p}_z$)
2	1	±1	$\frac{1}{2\sqrt{6}}\left(\frac{Z}{a}\right)^{3/2}\rho\mathrm{e}^{-\rho/2}$	$-\sqrt{\frac{3}{8\pi}}\sin\theta\mathrm{e}^{\pm\mathrm{i}\varphi}$	$2\mathrm{p}_{\pm1}$ (or $2\mathrm{p}_{x,y}$)
3	0	0	$3^{-5/2}\left(\frac{Z}{a}\right)^{3/2}\mathrm{e}^{-\rho/2}(6-6\rho+\rho^2)$	$\sqrt{\frac{1}{4\pi}}$	3s
3	1	0	$\frac{1}{9\sqrt{6}}\left(\frac{Z}{a}\right)^{3/2}\rho\mathrm{e}^{-\rho/2}(4-\rho)$	$\sqrt{\frac{3}{4\pi}}\cos\theta$	$3\mathrm{p}_0$ (or $3\mathrm{p}_z$)
3	1	±1	$\frac{1}{9\sqrt{6}}\left(\frac{Z}{a}\right)^{3/2}\rho\mathrm{e}^{-\rho/2}(4-\rho)$	$-\sqrt{\frac{3}{8\pi}}\sin\theta\mathrm{e}^{\pm\mathrm{i}\varphi}$	$3\mathrm{p}_{\pm1}$ (or $3\mathrm{p}_{x,y}$)
3	2	0	$\frac{1}{9\sqrt{30}}\left(\frac{Z}{a}\right)^{3/2}\rho^2\mathrm{e}^{-\rho/2}$	$\sqrt{\frac{5}{16\pi}}(3\cos^2\theta-1)$	$3\mathrm{d}_0$ (or $3\mathrm{d}_{z^2}$)
3	2	±1	$\frac{1}{9\sqrt{30}}\left(\frac{Z}{a}\right)^{3/2}\rho^2\mathrm{e}^{-\rho/2}$	$-\sqrt{\frac{15}{8\pi}}\sin\theta\cos\theta\mathrm{e}^{\pm\mathrm{i}\varphi}$	$3\mathrm{d}_{\pm1}$ (or $3\mathrm{d}_{xz,yz}$)
3	2	±2	$\frac{1}{9\sqrt{30}}\left(\frac{Z}{a}\right)^{3/2}\rho^2\mathrm{e}^{-\rho/2}$	$\sqrt{\frac{15}{32\pi}}\sin^2\theta\mathrm{e}^{\pm\mathrm{i}2\varphi}$	$3\mathrm{d}_{\pm2}$ (or $3\mathrm{d}_{xy,x^2-y^2}$)

Table 2.1: Quantum numbers, wave functions and symmetry designation of the lowest eigenstates of the hydrogen atom. Linear combinations of the complex-valued $R_{n\ell}(r)Y_{\ell m_\ell}(\theta,\varphi)$ can be formed that are real and correspond to the orbitals actually used by chemists with designations given in parentheses in the last column. $a = a_0\frac{m_\mathrm{e}}{\mu}$ and $\rho = \frac{2Z}{na}r$.

The energy eigenvalues given by Equation (2.3) do not depend on the quantum numbers ℓ and m_ℓ and have therefore a degeneracy factor of n^2. They form an infinite series which converges at $n=\infty$ to a value of 0. Positive energies thus correspond to situations where the electron is no longer bound to the nucleus, *i. e.*, to an ionization continuum. Expressing the energy relative to the lowest ($n=1$) level

$$E_{n\ell m_\ell} = hcZ^2R_M\left(1-\frac{1}{n^2}\right) = hcT_n, \tag{2.5}$$

one recognizes that the ionization energy of the 1s level is hcZ^2R_M, or, expressed as a term value in the wavenumber unit of cm^{-1}, $T_{n=\infty} = R_M$.

The functions $\Psi_{n\ell m_\ell}(r,\theta,\phi)$ represent orbitals and describe the bound states of one-electron atoms; the product $\Psi^*_{n\ell m_\ell}\Psi_{n\ell m_\ell} = |\Psi_{n\ell m_\ell}|^2$ represents the probability density of finding the electron at the position (r,θ,φ) and implies the following general behavior:

- The average distance between the electron and the nucleus is *proportional to* n^2, in accordance with Bohr's model of the hydrogen atom, which predicts that the classical radius of the electron orbit should grow with n as $a_0 n^2$, a_0 being the Bohr radius ($a_0 = 0.52917721092(17) \times 10^{-10}\,\mathrm{m}$).

- The probability of finding the electron in the immediate vicinity of the nucleus, *i. e.*, within a sphere of radius on the order of a_0, *decreases with* n^{-3}. This implies that all physical properties which depend on this probability, such as the excitation probability from the ground state, or the radiative decay rate to the ground state should also scale with n^{-3}.

The orbital angular momentum quantum number ℓ, which comes naturally in the solution of the Schrödinger equation of the hydrogen atom, is also a symmetry label of the corresponding quantum states. Indeed, the $2\ell+1$ functions $\Psi_{n\ell m_\ell}(r,\theta,\varphi)$ with $m_\ell = -\ell, -\ell+1, \ldots, \ell$ are designated by letters as s ($\ell=0$), p ($\ell=1$), d ($\ell=2$), f ($\ell=3$), g ($\ell=4$), with subsequent labels in alphabetical order, *i. e.*, h, i, k, l, etc. for $\ell = 5$, 6, 7, 8, etc. The distinction between electronic orbitals and electronic states is useful in polyelectronic atoms.
The operators $\hat{\vec{\ell}}^2$ and $\hat{\ell}_z$ describing the squared norm of the orbital angular momentum vector and its projection along the z axis commute with $\hat{H}$ and with each other. The spherical harmonics $Y_{\ell m_\ell}(\theta,\varphi)$ are thus also eigenfunctions of $\hat{\vec{\ell}}^2$ and $\hat{\ell}_z$ with eigenvalues given by the eigenvalue equations

$$\hat{\vec{\ell}}^2 Y_{\ell m_\ell}(\theta,\varphi) = \hbar^2 \ell(\ell+1) Y_{\ell m_\ell}(\theta,\varphi) \tag{2.6}$$

and

$$\hat{\ell}_z Y_{\ell m_\ell}(\theta,\varphi) = \hbar m_\ell Y_{\ell m_\ell}(\theta,\varphi). \tag{2.7}$$

2.1.2 Polyelectronic atoms

REMINDER: Exact and approximate separability of the Schrödinger equation

We consider a system of two particles described by the Hamiltonian:

$$\hat{H} = \hat{H}_1(\hat{p}_1, \vec{q}_1) + \hat{H}_2(\hat{p}_2, \vec{q}_2) \tag{2.8}$$

Each operator $\hat{H}_i$ only depends on the momentum operator $\hat{p}_i$ and coordinates $\vec{q}_i$ of particle i. In such a case, a solution of the Scrödinger equation

$$\hat{H}\,\Psi_n = E_n\,\Psi_n \tag{2.9}$$

can be written as a *product*

$$\Psi_n = \phi_{n_1,1}\phi_{n_2,2}, \tag{2.10}$$

and the eigenvalues as a *sum*

$$E_n = E_{n_1,1} + E_{n_2,2}. \tag{2.11}$$

Inserting Equation (2.10) and Equation (2.11) into Equation (2.9) one obtains:

$$\left(\hat{H}_1 + \hat{H}_2\right)\phi_{n_1,1}\phi_{n_2,2} = \left(E_{n_1,1} + E_{n_2,2}\right)\phi_{n_1,1}\phi_{n_2,2}, \tag{2.12}$$

i. e. $\hat{H}_1\phi_{n_1,1} = E_{n_1,1}\phi_{n_1,1}$ and $\hat{H}_2\phi_{n_2,2} = E_{n_2,2}\phi_{n_2,2}$.

In general the wavefunction of n non-interacting particles is the *product* of the one-particle wavefunctions and the total energy is the *sum* of the one-particle energies.

In many cases the Schrödinger equation is *nearly* separable. This is the case when

$$\hat{H} = \hat{H}_1(\hat{p}_1, \vec{q}_1) + \hat{H}_2(\hat{p}_2, \vec{q}_2) + \hat{H}', \tag{2.13}$$

where the expectation values of $\hat{H}'$ are much smaller than those of $\hat{H}_1$ and $\hat{H}_2$. The functions $\phi_{n_1,1}(\vec{q}_1)\phi_{n_2,2}(\vec{q}_2)$ are very similar to the exact eigenfunctions of $\hat{H}$ and serve as a good approximation for them. In such a case, *perturbation theory* is a good approach to improve the approximation.

The Hamiltonian for atoms with more than one electron can be written as follows:

$$\hat{H} = \sum_{i=1}^{N} \underbrace{\left(\frac{\hat{p}_i^2}{2m_\mathrm{e}} - \frac{Ze^2}{4\pi\varepsilon_0 r_i}\right)}_{\hat{h}_i} + \underbrace{\sum_{i=1}^{N}\sum_{j>i}^{N} \frac{e^2}{4\pi\varepsilon_0 r_{ij}}}_{\hat{H}'} + \hat{H}'' \ , \tag{2.14}$$

where $\hat{H}''$ represents all weak interactions not contained in $\hat{h}_i$ and $\hat{H}'$, cannot be solved analytically. If $\hat{H}'$ and $\hat{H}''$ in Equation (2.14) are neglected, $\hat{H}$ becomes separable in N

one-electron operators $\hat{h}_i(\hat{p}_i, q_i)$ with $\hat{h}_i(\hat{p}_i, q_i)\phi_j(q_i) = \epsilon_j\phi_j(q_i)$ (to simplify the notation, we use in the following the notation q_i instead of $\vec{q_i}$ to designate all spatial x_i, y_i, z_i and spin m_{s_i} coordinates of the polyelectron wave function)

$$\hat{H}_0 = \sum_{i=1}^{N} \hat{h}_i(\hat{p}_i, q_i), \tag{2.15}$$

with eigenfunctions

$$\Psi_k(q_1, \ldots, q_N) = \phi_{k_1}(q_1)\phi_{k_2}(q_2)\ldots\phi_{k_N}(q_N) \tag{2.16}$$

and eigenvalues

$$E_k = \epsilon_{k_1} + \epsilon_{k_2} + ... + \epsilon_{k_N}, \tag{2.17}$$

where $\phi_j(q_i) = R_{n_j\ell_j}(r_i)Y_{\ell_j m_{\ell_j}}(\theta_i, \varphi_i)\sigma_{m_{s_j}}$ represents a spin orbital with $\sigma_{m_{s_j}}$ being the spin part of the orbital, either α for $m_{s_j} = 1/2$ or β for $m_{s_j} = -1/2$.

The electron wave function in Equation (2.16) gives the occupation of the atomic orbitals and represents a given electron configuration *e. g.*, for the atom of lithium (Li), one gets: $\Psi_1(q_1, q_2, q_3) = 1s\alpha(q_1), 1s\beta(q_2), 2s\alpha(q_3)$. Neglecting the electron-repulsion term $\hat{H}'$ in Equation (2.14) is a very crude approximation, and it needs to be considered to get a realistic estimation of the eigenfunctions and eigenvalues of $\hat{H}$. A way to consider $\hat{H}'$ without affecting the product form of Equation (2.16) is to introduce, for each electron, a potential energy term describing the interaction with the mean field of all other electrons. Iteratively solving one-electron problems and modifying the mean-field potential term lead to the so-called "Hartree-Fock Self-Consistent Field" (HF-SCF) wave functions, which still have the form of Equation (2.16) for a single electronic configuration but now incorporate most effects of the electron-electron repulsion except their instantaneous correlation. Because polyelectronic atoms are also spherically symmetric the angular part of the improved orbitals can also be described by spherical harmonics $Y_{\ell m_\ell}(\theta_i, \varphi_i)$. However, the radial functions $R_{n\ell}(r_i)$ and the orbital energies (ϵ_j) differ from the hydrogenic case because of the electron-electron repulsion term $\hat{H}'$.

An empirical sequence of orbital energies can be determined that can be used to predict the *ground-state* configuration of most atoms in the periodic system using **Pauli's Aufbau-principle**:

$$\begin{aligned} &\epsilon_{1s} \leq \epsilon_{2s} \leq \epsilon_{2p} \leq \epsilon_{3s} \leq \epsilon_{3p} \leq \epsilon_{4s} \leq \epsilon_{3d} \leq \epsilon_{4p} \leq \\ &\epsilon_{5s} \leq \epsilon_{4d} \leq \epsilon_{5p} \leq \epsilon_{6s} \leq \epsilon_{4f} \leq \epsilon_{5d} \leq \epsilon_{6p} \leq \epsilon_{7s} \leq \\ &\epsilon_{5f} \leq \epsilon_{6d}. \end{aligned} \tag{2.18}$$

This sequence of orbital energies can be qualitatively explained by considering the shielding of the nuclear charge by electrons in inner shells and the decrease, with increasing value of ℓ, of the penetrating character of the orbitals.

For most purposes and in many atoms the product form of Equation (2.16) represents an adequate approximation of the N-electron wave function. However, Equation (2.16) is, not compatible with the generalized Pauli principle. Indeed, electrons have a half-integer spin quantum number ($s = 1/2$) and polyelectronic wave functions must be *antisymmetric* with respect to the exchange (permutation) of the coordinates of any pair of electrons. Equation (2.16) must therefore be antisymmetrized with respect to such an exchange of coordinates. This is achieved by writing the wave functions as determinants of the type:

$$\Psi(q_1, \ldots, q_N) = \frac{1}{\sqrt{N!}} \det \begin{vmatrix} \phi_{k_1}(q_1) & \phi_{k_1}(q_2) & \ldots & \phi_{k_1}(q_N) \\ \phi_{k_2}(q_1) & \phi_{k_2}(q_2) & \ldots & \phi_{k_2}(q_N) \\ \cdot & & & \\ \cdot & & & \\ \cdot & & & \\ \phi_{k_N}(q_1) & \ldots & \ldots & \phi_{k_N}(q_N) \end{vmatrix} \tag{2.19}$$

in which all ϕ_i are *different* spin orbitals. Such determinants are called **Slater determinants** and represent suitable N-electron wave functions which automatically fulfill the Pauli principle for fermions. Indeed, exchanging two columns in a determinant, *i. e.*, permuting the coordinates of two electrons, automatically changes the sign of the determinant. The determinant of a matrix with two identical rows is zero so that Equation (2.19) is also in accord with Pauli's exclusion principle, namely that any configuration with two electrons in the same spin orbital is forbidden. This is not surprising given that Pauli's exclusion principle can be regarded as a consequence of the generalized Pauli principle for fermions. The ground-state configuration of an atom can thus be obtained by filling the orbitals in order of increasing energy (see Equation (2.18)) with two electrons, one with $m_s = 1/2$, the other with $m_s = -1/2$, a procedure known as the Pauli's Aufbau-principle.

2.1.3 Singlet and triplet states

The generalized Pauli principle for fermions also restricts the number of possible wave functions associated with a given configuration, as illustrated with the ground electronic configuration of the carbon atom in the following example.

Example: C $(1s)^2(2s)^2(2p)^2$

Because the $(1s)^2$ and the $(2s)^2$ shells are fully occupied, only the $(2p)^2$ open subshell needs to be considered. There are six spin orbitals and therefore $6^2 = 36$ possible configurations $(2pm_\ell m_s)(2pm_{\ell'} m_{s'})$ with $m_\ell, m_{\ell'} = 0, \pm 1$ and $m_s, m_{s'} = \pm 1/2$, corresponding to the 36 entries of the table:

		Electron 1					
		$\phi_{2p1\alpha}$	$\phi_{2p1\beta}$	$\phi_{2p0\alpha}$	$\phi_{2p0\beta}$	$\phi_{2p-1\alpha}$	$\phi_{2p-1\beta}$
Electron 2	$\phi_{2p1\alpha}$	×		*			
	$\phi_{2p1\beta}$		×				
	$\phi_{2p0\alpha}$	*		×			
	$\phi_{2p0\beta}$				×		
	$\phi_{2p-1\alpha}$					×	
	$\phi_{2p-1\beta}$						×

Diagonal elements of the table (designated by a cross) are forbidden by the Pauli principle because both electrons are in the same spin orbital. According to Equation (2.19), each pair of symmetric entries with respect to the diagonal can be used to make one antisymmetric wave function. For example, the entries of the table marked by an asterisk (*) lead to the wave function

$$\Psi(q_1, q_2) = \frac{1}{\sqrt{2}} \left(\phi_{2p0\alpha}(q_1)\phi_{2p1\alpha}(q_2) - \phi_{2p1\alpha}(q_1)\phi_{2p0\alpha}(q_2)\right), \tag{2.20}$$

which is antisymmetric with respect to permutation of q_1 and q_2 and thus fulfills the generalized Pauli principle for fermions, and to one symmetric wave function

$$\Psi(q_1, q_2) = \frac{1}{\sqrt{2}} \left(\phi_{2p0\alpha}(q_1)\phi_{2p1\alpha}(q_2) + \phi_{2p1\alpha}(q_1)\phi_{2p0\alpha}(q_2)\right) \tag{2.21}$$

which is forbidden by the Pauli principle. In total there are 15 wave functions for the $(2p)^2$ configuration that fulfill the Pauli principle. Not all of these 15 wave functions correspond to states of the same energy.

For an excited configuration with two unpaired electrons such as He $(1s)^1(2s)^1$, the Pauli principle does not impose any restriction, because the two electrons are in different orbitals. However, the electrostatic repulsion between the two electrons leads to an **energetic splitting** of the possible states. In this configuration, four spin orbitals (1sα, 1sβ, 2sα, and 2sβ) need to be considered, because each electron can be either in the 1s or the 2s orbital with either $m_s = 1/2$ or $m_s = -1/2$. Four antisymmetrized functions fulfilling the Pauli principle result, which can be represented as products of a symmetric/antisymmetric spatial part depending on the x_i, y_i and z_i coordinates of the two electrons ($i = 1, 2$) and an

antisymmetric/symmetric spin part (T= triplet, S=singlet):

$$\frac{1}{\sqrt{2}}\left(1s(1)2s(2) - 1s(2)2s(1)\right)\alpha(1)\alpha(2) = \Psi_{T,M_S=1} \quad (2.22)$$

$$\frac{1}{\sqrt{2}}\left(1s(1)2s(2) - 1s(2)2s(1)\right)\beta(1)\beta(2) = \Psi_{T,M_S=-1} \quad (2.23)$$

$$\frac{1}{\sqrt{2}}\left(1s(1)2s(2) - 1s(2)2s(1)\right)\frac{1}{\sqrt{2}}\left[\alpha(1)\beta(2) + \alpha(2)\beta(1)\right] = \Psi_{T,M_S=0} \quad (2.24)$$

$$\frac{1}{\sqrt{2}}\left(1s(1)2s(2) + 1s(2)2s(1)\right)\frac{1}{\sqrt{2}}\left(\alpha(1)\beta(2) - \alpha(2)\beta(1)\right) = \Psi_{S,M_S=0}, \quad (2.25)$$

where the notation $1s(i)\alpha(i)$ has been used to designate electron i being in the 1s orbital with spin projection quantum number $m_s = 1/2$.

The first three functions (Equations (2.22), (2.23) and (2.24)), with $M_S = m_{s_1} + m_{s_2} = \pm 1, 0$, have an antisymmetric spatial part and a symmetric electron-spin part with respect to the permutation of the two electrons. These three functions represent the three components of a triplet ($S = 1$) state. The fourth function has a symmetric spatial and an antisymmetric electron-spin part with $M_S = 0$ and represents a singlet ($S = 0$) state. These results are summarized in Tables 2.2 and 2.3, where the spin part of the wave functions are designated with an superscript "S" and the spatial parts with a superscript "R". The subscripts "a" and "s" indicate whether the functions are symmetric or antisymmetric with respect to the permutation of the coordinates of the two electrons.

$\Psi^{\mathrm{S}}_{(\mathrm{s})}(m_1, m_2)$	$\alpha(1)\alpha(2)$	$M_S = 1$	$S = 1$(triplet)
	$\frac{1}{\sqrt{2}}(\alpha(1)\beta(2) + \alpha(2)\beta(1))$	$M_S = 0$	
	$\beta(1)\beta(2)$	$M_S = -1$	
$\Psi^{\mathrm{S}}_{(\mathrm{a})}(m_1, m_2)$	$\frac{1}{\sqrt{2}}(\alpha(1)\beta(2) - \alpha(2)\beta(1))$	$M_S = 0$	$S = 0$(singlet)

Table 2.2: Permutationally symmetric and antisymmetric two-electron spin functions

$\Psi^{\mathrm{R}}_{(\mathrm{s})}(q_1, q_2)$	$\frac{1}{\sqrt{2}}(\phi_1(1)\phi_2(2) + \phi_1(2)\phi_2(1))$	(singlet)
$\Psi^{\mathrm{R}}_{(\mathrm{a})}(q_1, q_2)$	$\frac{1}{\sqrt{2}}(\phi_1(1)\phi_2(2) - \phi_1(2)\phi_2(1))$	(triplet)

Table 2.3: Permutationally symmetric and antisymmetric two-electron spatial functions

The contribution to the energy of the electron-repulsion term $\hat{H}' = \frac{e^2}{4\pi\varepsilon_0 r_{12}}$ in Equation (2.14) can be evaluated in the first order of perturbation theory as:

$$\begin{aligned}\frac{e^2}{8\pi\varepsilon_0}\langle 1s(1)2s(2) - 1s(2)2s(1)|\frac{1}{r_{12}}|1s(1)2s(2) - 1s(2)2s(1)\rangle &= \frac{e^2}{8\pi\epsilon_0}[\langle 1s(1)2s(2)|\frac{1}{r_{12}}|1s(1)2s(2)\rangle \\ &\quad +\langle 1s(2)2s(1)|\frac{1}{r_{12}}|1s(2)2s(1)\rangle \\ &\quad -\langle 1s(1)2s(2)|\frac{1}{r_{12}}|1s(2)2s(1)\rangle \\ &\quad -\langle 1s(2)2s(1)|\frac{1}{r_{12}}|1s(1)2s(2)\rangle] \\ &= \frac{1}{2}\left(J_{12} + J_{21} - K_{12} - K_{21}\right) \\ &= J_{12} - K_{12} \qquad (2.26)\end{aligned}$$

for the triplet state, and as

$$\frac{e^2}{8\pi\varepsilon_0}\langle 1s(1)2s(2) + 1s(2)2s(1)|\frac{1}{r_{12}}|1s(1)2s(2) + 1s(2)2s(1)\rangle = J_{12} + K_{12} \qquad (2.27)$$

for the singlet state. In Equations (2.26) and (2.27), the integral $J_{12} = J_{21}$ and $K_{12} = K_{21}$ represent so-called **Coulomb** and **exchange integrals**, respectively. The Coulomb integral can be interpreted as the energy arising from the repulsion between the electron clouds of the 1s and 2s electrons. The exchange integral results from the repulsion between the two electron having "exchanged" their orbitals.

Because J_{12} and K_{12} are both positive in this case, the *triplet state lies lower in energy than the singlet state* by twice the exchange integral. The energy splitting between the singlet and triplet states can therefore be formally viewed as resulting from an electrostatic (including exchange) coupling of the motion of the two electrons with spin vectors $\vec{s}_1$ and $\vec{s}_2$, resulting in states of total spin angular momentum $\vec{S} = \vec{s}_1 + \vec{s}_2$ with $S = 1$ for the triplet state, and $S = 0$ for the singlet state.

These considerations can easily be generalized to situations with more than two unpaired electrons. In atoms with configurations with three unpaired electrons, such as, for instance, N ($(1s)^2(2s)^2(2p)^3$), quartet ($S = 3/2$) and doublet ($S = 1/2$) states result.

2.1.4 Terms and term symbols in atoms: LS and jj coupling

For all atoms extensive lists of term values are tabulated (see, *e. g.*, C.E. Moore, Atomic Energy Levels, in reading list). To understand how the different terms arise and derive the term symbols used to label them, it is necessary to understand how the different orbital and spin angular momenta in an atom are coupled by electromagnetic interactions and in which

sequence the angular momentum vectors are added to form the total angular momentum vector $\vec{J}$. This can be achieved by ordering the different interactions according to their relative strengths and by adding the angular momentum vectors that are most strongly coupled first. Each angular momentum vector can be described quantum mechanically by eigenvalue equations of the type of Equations (2.6) and (2.7), *e. g.*,

$$\hat{\vec{S}}^2|SM_S\rangle = \hbar^2 S(S+1)|SM_S\rangle, \tag{2.28}$$

$$\hat{S}_z|SM_S\rangle = \hbar M_S|SM_S\rangle, \tag{2.29}$$

$$\hat{\vec{L}}^2|LM_L\rangle = \hbar^2 L(L+1)|LM_L\rangle, \tag{2.30}$$

$$\hat{L}_z|LM_L\rangle = \hbar M_L|LM_L\rangle, \tag{2.31}$$

$$\hat{\vec{J}}^2|JM_J\rangle = \hbar^2 J(J+1)|JM_J\rangle, \tag{2.32}$$

$$\hat{J}_z|JM_J\rangle = \hbar M_J|JM_J\rangle. \tag{2.33}$$

In the absence of coupling between the different angular momenta, all quantum numbers arising from eigenvalue equations of this type are good quantum numbers. In the presence of couplings between the different angular momenta, however, only a subset of these quantum numbers remain good quantum numbers, and the actual subset of good quantum numbers depends on the hierarchy of coupling strengths (R. Zare, Angular Momentum, in reading list).

Two limiting cases of angular momentum coupling hierarchy are used to label the terms of atoms: the LS coupling hierarchy, which adequately describes the ground state of almost all atoms except the heaviest ones, and the jj coupling hierarchy, which is less frequently encountered and becomes important in the description of the heaviest atoms and of electronically excited states.

The LS coupling hierarchy

$\vec{L} = \sum_{i=1}^{N} \vec{\ell}_i$: Strong coupling of orbital angular momenta resulting from electrostatic interactions

$\vec{S} = \sum_{i=1}^{N} \vec{s}_i$: Strong coupling of spins resulting from exchange terms in the electrostatic interaction (see Equations (2.26) and (2.27))

$\vec{J} = \vec{L} + \vec{S}$: Weaker coupling between $\vec{S}$ and $\vec{L}$ resulting from the spin-orbit interaction (relativistic effect)

In LS coupling, one obtains the possible terms by first adding vectorially the orbital angular

momenta $\vec{\ell}_i$ of the electrons to form a resultant total orbital angular momentum $\vec{L}$. Then, the total electron spin $\vec{S}$ is determined by vectorial addition of the spins $\vec{s}_i$ of all electrons. Finally, the total angular momentum $\vec{J}$ is determined by adding vectorially $\vec{S}$ and $\vec{L}$. For a two-electron system, one obtains:

$$\vec{L} = \vec{\ell}_1 + \vec{\ell}_2; \quad L = |\ell_1 - \ell_2|, |\ell_1 - \ell_2| + 1, \ldots, \ell_1 + \ell_2 \tag{2.34}$$

$$M_L = m_{\ell_1} + m_{\ell_2} = -L, -L+1, \ldots, L \tag{2.35}$$

$$\vec{S} = \vec{s}_1 + \vec{s}_2; \quad S = 1, 0 \tag{2.36}$$

$$M_S = m_{s_1} + m_{s_2} = -S, -S+1, \ldots, S \tag{2.37}$$

$$\vec{J} = \vec{L} + \vec{S}; \quad J = |L - S|, |L - S| + 1, \ldots, L + S \tag{2.38}$$

$$M_J = M_S + M_L = -J, -J+1, \ldots, J. \tag{2.39}$$

The angular momentum quantum numbers L, S and J that arise in Equations (2.34), (2.36), and (2.38) from the addition of the pairs of coupled vectors $(\vec{\ell}_1, \vec{\ell}_2)$, $(\vec{s}_1, \vec{s}_2)$ and $(\vec{L}, \vec{S})$, respectively, can be derived from angular momentum algebra as explained in most quantum mechanics textbooks.

The different terms (L, S, J) that are obtained for the possible values of L, S and J in Equations (2.34), (2.36), and (2.38) are written in compact form as **term symbols**

$$^{2S+1}L_J. \tag{2.40}$$

However, not all terms that are predicted by Equations (2.34), (2.36), and (2.38) are allowed by the Pauli principle. This is best explained by deriving the possible terms of the C $(1s)^2(2s)^2(2p)^2$ configuration in the following example.

Example: C $(1s)^2(2s)^2(2p)^2$. Only the partially filled 2p subshell needs to be considered. In this case $l_1 = 1$, $l_2 = 1$ and $s_1 = s_2 = 1/2$. From Equations (2.34), (2.36), and (2.38) one obtains, neglecting the Pauli principle:

$$\begin{aligned} L &= 0(\mathrm{S}), 1(\mathrm{P}), 2(\mathrm{D}) \\ S &= 0(\text{singlet}), 1(\text{triplet}) \\ J &= 0, 1, 2, 3 \end{aligned}$$

which leads to the following terms:

Term	$^1S_0$	$^3S_1$	$^1P_1$	$^3P_0$	$^3P_1$	$^3P_2$	$^1D_2$	$^3D_1$	$^3D_2$	$^3D_3$
Degeneracy factor $g_J = 2J+1$	1	3	3	1	3	5	5	3	5	7

Taking the $(2J + 1)$ degeneracy factor of each term (which corresponds to all possible values of M_J), a total of 36 states result. As discussed above, only 15 states are allowed by the Pauli principle for the configuration $(1s)^2(2s)^2(2p)^2$. The terms allowed by the Pauli principle can be determined by first finding the M_L, M_S and M_J values resulting from all 15 possible occupations of the six 2p spin-orbitals with the two electrons in *different* spin orbitals, as explained in the following table:

El. 1	El. 2	M_L	M_S	M_J
$\phi_{2p1\alpha}$	$\phi_{2p1\beta}$	2	0	2
	$\phi_{2p0\alpha}$	1	1	2
	$\phi_{2p0\beta}$	1	0	1
	$\phi_{2p-1\alpha}$	0	1	1
	$\phi_{2p-1\beta}$	0	0	0
$\phi_{2p1\beta}$	$\phi_{2p0\alpha}$	1	0	1
	$\phi_{2p0\beta}$	1	-1	0
	$\phi_{2p-1\alpha}$	0	0	0
	$\phi_{2p-1\beta}$	0	-1	-1
$\phi_{2p0\alpha}$	$\phi_{2p0\beta}$	0	0	0
	$\phi_{2p-1\alpha}$	-1	1	0
	$\phi_{2p-1\beta}$	-1	0	-1
$\phi_{2p0\beta}$	$\phi_{2p-1\alpha}$	-1	0	-1
	$\phi_{2p-1\beta}$	-1	-1	-2
$\phi_{2p-1\alpha}$	$\phi_{2p-1\beta}$	-2	0	-2

The maximum value of M_L is 2 and occurs only in combination with $M_S = 0$. This implies a ^{1}D term with five M_J components corresponding to $(M_L\ M_S)$ = (2 0), (1 0), (0 0), (-1 0) and (-2 0). Eliminating these entries from the table, the remaining entry with the highest M_L value has $M_L = 1$ and comes in combination with a maximal M_S value of 1. We can conclude that the corresponding term is ^{3}P (consisting of $^3P_0$, $^3P_1$ and $^3P_2$). There are 9 components corresponding to $(M_L\ M_S)$ = (1 1), (1 0), (1 -1), (0 1), (0 0), (0 -1), (-1 1), (-1 0) and (-1 -1). Eliminating these entries from the table, only one component remains, (0 0), which corresponds to a $^1S_0$ state. The terms corresponding to the $(2p)^2$ configuration allowed by the Pauli principle are therefore $^1D_2$, $^3P_2$, $^3P_1$, $^3P_0$ and $^1S_0$. As in the case of the He $(1s)^1(2s)^1$ configuration discussed above, the electrostatic exchange interaction favors the triplet state over the singlet states.

The lowest energy term of the ground electronic configuration of almost all atoms can be predicted using three empirical rules, know as **Hund's rules** in honor of the physicist Friedrich Hund (1896 – 1997). These rules state that

1. The lowest term is that with the highest value of the total spin angular momentum quantum number S.

2. If several terms have the same value of S, the term with the highest value of the total angular momentum quantum number L lies lowest in energy.

3. If the lowest term is such that both L and S are nonzero, the ground state is the term

component with $J = |L - S|$ if the partially filled subshell is *less than half full*, and the term component with $J = L + S$ if the partially filled subshell is *more than half full*.

According to Hund's rules, the ground state of C is the term component $^3P_0$, and the ground state of F is the term component $^2P_{3/2}$, in agreement with experimental results. Hund's rules do not reliably predict the energetic ordering of electronically excited states.

The energy level splittings of the components of a term ^{2S+1}L can be described by considering the effect of the effective **spin-orbit operator**

$$\hat{H}_{\mathrm{SO}} = \frac{hcA}{\hbar^2} \hat{\vec{L}} \cdot \hat{\vec{S}} \tag{2.41}$$

on the basis functions $|LSJ\rangle$ with $\hat{\vec{J}} = \hat{\vec{L}} + \hat{\vec{S}}$. In Equation (2.41), the spin-orbit coupling constant A is expressed in cm^{-1}. From $\hat{\vec{J}}^2 = \hat{\vec{L}}^2 + \hat{\vec{S}}^2 + 2\hat{\vec{L}} \cdot \hat{\vec{S}}$ one finds

$$\hat{\vec{L}} \cdot \hat{\vec{S}} = \frac{1}{2} \left[\hat{\vec{J}}^2 - \hat{\vec{L}}^2 - \hat{\vec{S}}^2 \right]. \tag{2.42}$$

The diagonal matrix elements of $\hat{H}_{\mathrm{SO}}$, which represent the first-order corrections to the energies in a perturbation theory treatment, are

$$\langle LSJ|\hat{H}_{\mathrm{SO}}|LSJ\rangle = \frac{1}{2} hcA[J(J+1) - L(L+1) - S(S+1)], \tag{2.43}$$

from which one sees that two components of a term with J and $J+1$ are separated in energy by $hcA(J+1)$. Hund's third rule implies that the spin-orbit coupling constant A is positive in ground terms arising from less than half-full subshells and negative in ground terms arising from more than half-full subshells.

To illustrate the main conclusions of this subsection, Figure 2.1 shows schematically by which interactions the 15 states of the ground-state configuration of C can be split. The strong electrostatic interactions (including exchange) lead to a splitting into three terms ^3P, ^1D and ^1S. The weaker spin-orbit interaction splits the ground ^3P term into three components $^3P_0$, $^3P_1$ and $^3P_2$. Each term component can be further split into $(2J+1)$ M_J levels by an external magnetic field, an effect known as the Zeeman effect.

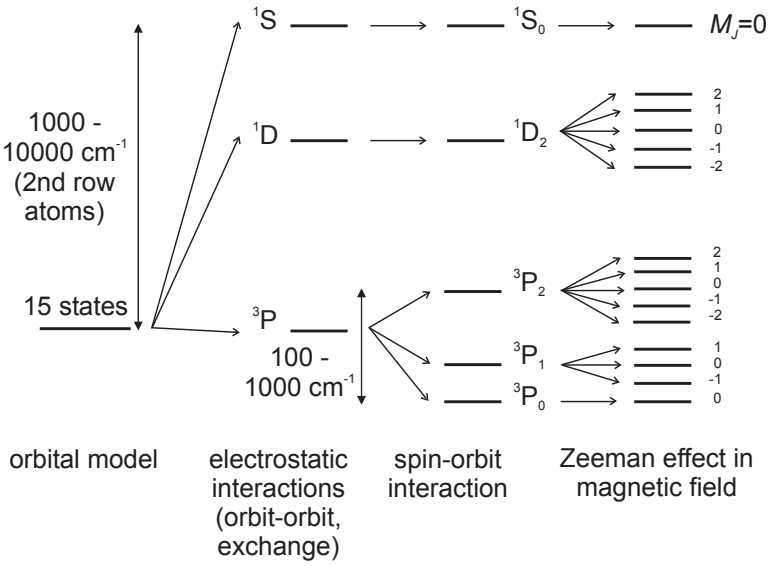

Figure 2.1: Schematic energy level structure of the $(2p)^2$ configuration in LS coupling.

The jj coupling hierarchy

$\vec{l}_i + \vec{s}_i = \vec{j}_i$: Strong spin-orbit coupling

$\sum \vec{j}_i = \vec{J}$: Weaker electrostatic coupling.

In heavy atoms, relativistic effects become so large that the spin-orbit interaction can become comparable in strength, or even larger, than the electrostatic (including exchange) interactions that are dominant in the lighter atoms. In jj coupling, the dominant interaction is the spin-orbit coupling between $\vec{l}_i$ and $\vec{s}_i$. The possible terms are obtained by first adding vectorially the orbital angular momentum vector $\vec{l}_i$ and the electron spin vector $\vec{s}_i$ of each electron (index i) to form a resultant electronic angular momentum $\vec{j}_i$. The total electronic angular momentum $\vec{J}$ results from the vectorial addition of all $\vec{j}_i$.

For a two electron system, one obtains, using the same angular momentum addition rules that led to Equations (2.34), (2.36), and (2.38):

$$\vec{j}_1 = \vec{l}_1 + \vec{s}_1; \qquad j_1 = |l_1 - \frac{1}{2}|,\ l_1 + \frac{1}{2} \tag{2.44}$$

$$m_{j_1} = m_{l_1} + m_{s_1} = -j_1, -j_1 + 1, \ldots, j_1 \tag{2.45}$$

$$\vec{j}_2 = \vec{l}_2 + \vec{s}_2; \qquad j_2 = |l_2 - \frac{1}{2}|,\ l_2 + \frac{1}{2} \tag{2.46}$$

$$m_{j_2} = m_{l_2} + m_{s_2} = -j_2, -j_2 + 1, \ldots, j_2 \tag{2.47}$$

$$\vec{J} = \vec{j}_1 + \vec{j}_2; \qquad J = |j_1 - j_2|, |j_1 - j_2| + 1, \ldots, j_1 + j_2 \tag{2.48}$$

$$M_J = m_{j_1} + m_{j_2} = -J, -J + 1, \ldots, J. \tag{2.49}$$

The total orbital and spin angular momentum quantum numbers L and S are no longer defined in jj coupling. Instead, the terms are now specified by a different set of angular momentum quantum numbers: the total angular momentum j_i of all electrons (index i) in partially filled subshells and the total angular momentum quantum number J of the atom. A convenient way to label the terms is $(j_1, j_2, \ldots, j_N)_J$.

Example: The $(n\mathrm{p})^1((n+1)\mathrm{s})^1$ excited configuration:

LS coupling: $S = 0, 1$; $L = 1$. Termsymbols: $^1\mathrm{P}_1$, $^3\mathrm{P}_{0,1,2}$, which give rise to 12 states.

jj coupling: $l_1 = 1, s_1 = \frac{1}{2}, j_1 = \frac{1}{2}, \frac{3}{2}$ and $l_2 = 0, s_2 = \frac{1}{2}, j_2 = \frac{1}{2}$. Termsymbols: $[(j_1, j_2)_J]$: $(\frac{1}{2}, \frac{1}{2})_0; (\frac{1}{2}, \frac{1}{2})_1; (\frac{3}{2}, \frac{1}{2})_1; (\frac{3}{2}, \frac{1}{2})_2$, which also gives rise to 12 states.

The evolution from LS coupling to jj coupling can be observed by looking at the evolution of the energy level structure associated with a given configuration as one moves down a column in the periodic table. Figure 2.2 illustrates schematically how the energy levels arising from the $(n\mathrm{p})^1((n+1)\mathrm{s})^1$ excited configuration are grouped according to LS coupling for $n = 2$ and 3 (C and Si) and according to jj coupling for $n = 6$ (Pb). The main splitting between the $(1/2, 1/2)_{0,1}$ and the $(3/2, 1/2)_{1,2}$ states of Pb is actually much larger than the splitting between the ^{3}P and ^{1}P terms. Figure 2.2 is a so-called correlation diagram, which represents how the energy level structure of a given system (here the states of the $(n\mathrm{p})^1((n+1)\mathrm{s})^1$ configuration) evolves as a function of one or more system parameters (here the magnitude of the spin-orbit and electrostatic interactions). States with the same values of all good quantum numbers (here J) are usually connected by lines and do not cross in a correlation diagram.

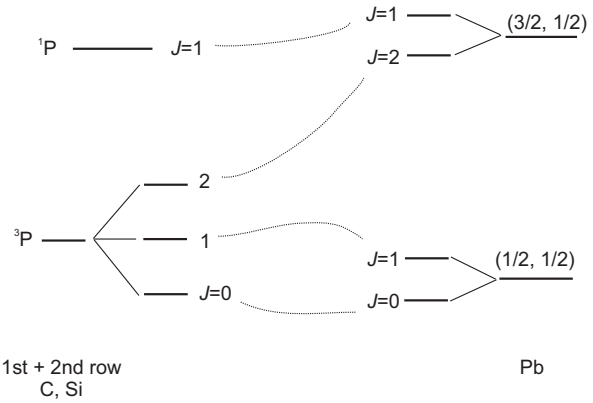

Figure 2.2: Correlation diagram depicting schematically, and not to scale, how the term values for the $(n\mathrm{p})((n+1)\mathrm{s})$ configuration evolve from C, for which the LS coupling limit represents a good description, to Pb, the level structure of which is more adequately described by the jj coupling limit.

The actual evolution of the energy level structure in the series C, Si, Ge, Sn and Pb, drawn to scale in Figure 2.3 using reference data on atomic term values, enables one to see quantitatively the effects of the gradual increase of the spin-orbit coupling. For the comparison, the zero point of the energy scale was placed at the center of gravity of the energy level structure. In C, the spin-orbit interaction is weaker than the electrostatic interactions, and the spin-orbit splittings of the ^{3}P state are hardly recognizable on the scale of the figure. In Pb, it is stronger than the electrostatic interactions and determines the main splitting of the energy level structure.

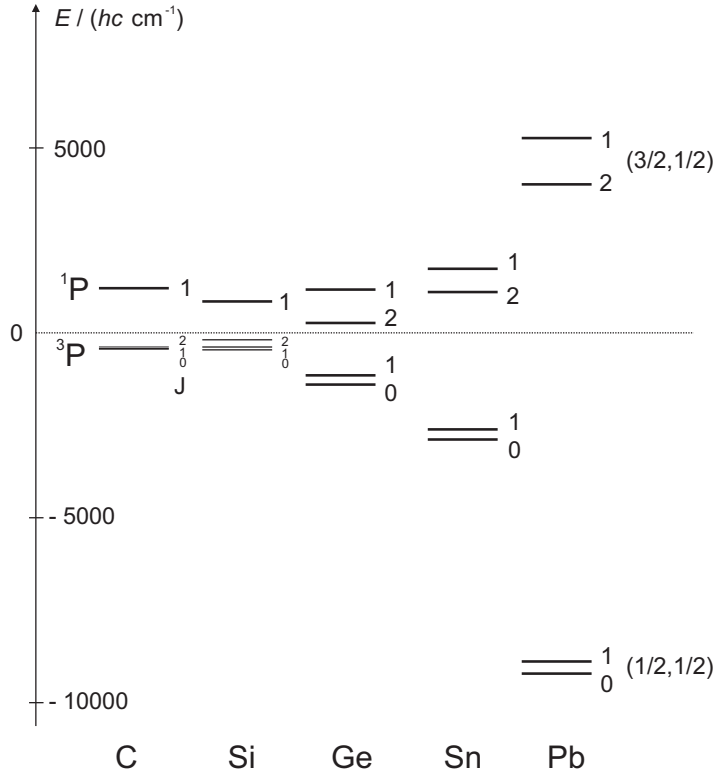

Figure 2.3: Evolution from LS coupling to jj coupling with the example of the term values of the $(np)^1((n+1)s)^1$ configuration of C, Si, Ge, Sn and Pb. The terms symbols are indicated without the value of J on the left-hand side for the LS coupling limit and on the right-hand side for the jj coupling limit. The values of J are indicated next to the horizontal bars corresponding to the positions of the energy levels.

2.1.5 Hyperfine coupling

Magnetic moments arise in systems of charged particles with nonzero angular momenta to which they are proportional. In the case of the orbital angular momentum of an electron, the

origin of the magnetic moment can be understood by considering the similarity between the orbital motion of an electron in an atom and a "classical" current generated by an electron moving with velocity v in a circular loop or radius r. The magnetic moment is equal to

$$\vec{\mu} = -\frac{e}{2m_\mathrm{e}}\vec{r} \times m_\mathrm{e}\vec{v} = -\frac{e}{2m_\mathrm{e}}\vec{\ell} = \gamma\vec{\ell}. \tag{2.50}$$

For the orbital motion of an electron in an atom, Equation (2.50) can be written using the correspondence principle as

$$\hat{\vec{\mu}} = \gamma\hat{\vec{\ell}} = -\frac{\mu_\mathrm{B}}{\hbar}\hat{\vec{\ell}}, \tag{2.51}$$

where $\gamma = -e/(2m_\mathrm{e})$ represents the magnetogyric ratio of the orbital motion and $\mu_\mathrm{B} = e\hbar/(2m_\mathrm{e}) = 9.27400968(20) \times 10^{-24}\,\mathrm{J\,T^{-1}}$ is the Bohr magneton. By analogy, similar equations can be derived for all other momenta. The electron spin $\vec{s}$ and the nuclear spin $\vec{I}$, for instance, give rise to the magnetic moments

$$\hat{\vec{\mu}}_s = -g_\mathrm{e}\gamma\hat{\vec{s}} = g_\mathrm{e}\frac{\mu_\mathrm{B}}{\hbar}\hat{\vec{s}}, \tag{2.52}$$

and

$$\hat{\vec{\mu}}_I = \gamma_I\hat{\vec{I}} = g_I\frac{\mu_\mathrm{N}}{\hbar}\hat{\vec{I}}, \tag{2.53}$$

respectively, where g_e is the so-called g **value of the electron** ($g_\mathrm{e} = -2.0023193043622(15)$), γ_I is the **magnetogyric ratio** of the nucleus, $\mu_\mathrm{N} = e\hbar/(2m_\mathrm{p}) = 5.05078353(11)\times10^{-27}\,\mathrm{J\,T^{-1}}$ is the nuclear magneton ($m_\mathrm{p} = 1.672621777(74) \times 10^{-27}\,\mathrm{kg}$ is the mass of the proton), and g_I is the nuclear g factor ($g_\mathrm{p} = 5.585$ for the proton). Because $\mu_\mathrm{N}/\mu_\mathrm{B} = m_\mathrm{e}/m_\mathrm{p}$, the magnetic moments resulting from the electronic orbital and spin motions are typically 2 to 3 orders of magnitude larger than the magnetic dipole moments (and higher moments) of nuclear spins. The spin-orbit interaction is in general much stronger than the interactions involving nuclear spins. The hyperfine interaction can therefore be described as an interaction between $\vec{I}$, with magnetic moment $(g_I\mu_\mathrm{N}/\hbar)\hat{\vec{I}}$, and $\vec{J}$, with magnetic moment

$$\hat{\vec{\mu}}_J = g_J\gamma\hat{\vec{J}}, \tag{2.54}$$

rather than as two separate interactions of $\vec{I}$ with $\vec{L}$ and $\vec{S}$. In Equation (2.54), g_J is the g factor of the LS-coupled state, also called Landé g factor, and is given in good approximation by

$$g_J = 1 + \frac{J(J+1) + S(S+1) - L(L+1)}{2J(J+1)}. \tag{2.55}$$

The hyperfine interaction results in a total angular momentum vector $\vec{F}$ of norm $|\vec{F}| = \hbar\sqrt{F(F+1)}$ and z-axis projection $\hbar M_F$. The possible values of the quantum numbers F and M_F can be determined using the usual angular momentum addition rules:

$$F = |J - I|,\ |J - I| + 1, \ldots, J + I, \tag{2.56}$$

and

$$M_F = -F,\ -F + 1, \ldots, F. \tag{2.57}$$

The hyperfine contribution to $\hat{H}$ arising from the interaction of $\hat{\vec{\mu}}_J$ and $\hat{\vec{\mu}}_I$ is one of the terms included in $\hat{H}''$ in Equation (2.14) and is proportional to $\hat{\vec{\mu}}_I \cdot \hat{\vec{\mu}}_J$, and thus to $\hat{\vec{I}} \cdot \hat{\vec{J}}$. Following the same argument as that used to derive Equation (2.43), one obtains

$$\hat{\vec{I}} \cdot \hat{\vec{J}} = \frac{1}{2}\left[\hat{\vec{F}}^2 - \hat{\vec{I}}^2 - \hat{\vec{J}}^2\right] \tag{2.58}$$

with $\hat{\vec{F}} = \hat{\vec{I}} + \hat{\vec{J}}$ and $\hat{\vec{F}}^2 = \hat{\vec{I}}^2 + \hat{\vec{J}}^2 + 2\hat{\vec{I}} \cdot \hat{\vec{J}}$. The hyperfine energy shift of state $|IJF\rangle$ is therefore

$$\langle IJF|\frac{ha}{\hbar^2}\hat{\vec{I}} \cdot \hat{\vec{J}}|IJF\rangle = \frac{ha}{2}\left[F(F+1) - I(I+1) - J(J+1)\right] \tag{2.59}$$

as can be derived from Equation (2.58) and the eigenvalues of $\hat{\vec{F}}^2$, $\hat{\vec{I}}^2$ and $\hat{\vec{J}}^2$. In Equation (2.59), a is the hyperfine coupling constant in Hz. Note that choosing to express A in cm^{-1} and a in Hz is the reason for the additional factor of c in Equation (2.41). Examples of the fine and hyperfine structure of atoms will be given in Section 2.2.

2.2 Atomic spectra

2.2.1 Transition moments and selection rules

The intensity $I(\nu_{\mathrm{fi}})$ of a transition between an initial state of an atom or a molecule with wave function Ψ_{i} and energy E_{i} and a final state with wave function Ψ_{f} and energy E_{f} is proportional to the square of the matrix element $\hat{V}_{\mathrm{fi}}$, where the matrix $\hat{V}$ represents the operator describing the interaction between the radiation field and the atom or the molecule

$$I(\nu_{\mathrm{fi}}) \propto |\langle \Psi_{\mathrm{f}}|\hat{V}|\Psi_{\mathrm{i}}\rangle|^2 = \langle \mathrm{f}|\hat{V}|\mathrm{i}\rangle^2 = \hat{V}_{\mathrm{if}}^2. \tag{2.60}$$

The transition is observed at the frequency $\nu_{\mathrm{fi}} = |E_{\mathrm{f}} - E_{\mathrm{i}}|/h$.

A selection rule enables one to predict whether a transition can be observed or not on the basis of symmetry arguments. If $\langle \Psi_{\mathrm{f}}|\hat{V}|\Psi_{\mathrm{i}}\rangle = 0$, the transition f $\leftarrow$ i is said to be "forbidden",

i. e., not observable; if $\langle \Psi_\mathrm{f} | \hat{V} | \Psi_\mathrm{i} \rangle \neq 0$, the transition f $\leftarrow$ i is said to be "allowed".

The interaction between atoms or molecules and electromagnetic radiation within the dipole approximation is given by

$$\hat{V} = -\hat{\vec{M}} \cdot \vec{E}. \tag{2.61}$$

In the case of linearly polarized radiation, the electric field vector, defined in the laboratory-fixed (X, Y, Z) frame, is $(0, 0, E)$, and, therefore, $\hat{V} = -\hat{M}_Z E$. When studying the spectra of atoms, the laboratory-fixed (or space-fixed) reference frame is the only relevant frame, because it can always be chosen to coincide with an internal, "atom-fixed" reference frame. Indeed, the point-like nature of the nucleus implies that there are no rotations of the nuclear framework. For this reason, atomic spectra are simpler to treat than molecular spectra.

Selection rules for atomic transitions can be easily derived if the electron spin and orbital motions can be separated. The laboratory-fixed reference frame is the only relevant frame when determining selection rules for atoms. The X, Y and Z components of the electric-dipole-moment operator $\hat{\vec{M}}$ transform as the components X, Y, Z of the position operator $\vec{r}$ so that the single-photon transition moment is $\langle \Psi' | \hat{\vec{M}}_k | \Psi'' \rangle$ with $k = X, Y, Z$.

This property leads to the following selection rules:

The angular momentum selection rules

Within the dipole approximation, the photon can only exchange up to one unit of angular momentum with an atom or molecule (in the electric quadrupole approximation, up to two units can be exchanged): $\vec{J}_\mathrm{f} = \vec{J}_\mathrm{i} + \vec{1}$. Thus $J_\mathrm{f} = J_\mathrm{i}, J_\mathrm{i} \pm 1$ or

$$\Delta J = 0, \pm 1 \quad \text{with} \quad 0 \nleftrightarrow 0. \tag{2.62}$$

Because the transition moment operator does not act on the electron spin variable, one finds within the LS coupling scheme (only approximate scheme neglecting spin-orbit coupling between $\vec{l}_k$ and $\vec{s}_k$, see Section 2.1.4)

$$\Delta S = 0 \quad \text{and} \tag{2.63}$$

$$\Delta L = 0, \pm 1, \ 0 \nleftrightarrow 0. \tag{2.64}$$

Whenever electron-correlation effects are negligible and the electronic wave function can be represented as a single determinant (see Equation (2.19)), absorption of a single photon leads to a final electronic state differing from the initial one by a single spin-orbital, say $\phi_{n\ell m_\ell}(r, \theta, \varphi) = R_{n\ell}(r) Y_{\ell m_\ell}(\theta, \varphi)$. The transition moment can then be factorized using the

relation $z = r\cos(\theta)$ for radiation linearly polarized along $\vec{z}$:

$$I(\nu_{\text{fi}}) \propto \left|\langle\phi_{n'\ell'm'_\ell}|\hat{\vec{M}}|\phi_{n''\ell''m''_\ell}\rangle\right|^2 = \left|\langle R_{n'\ell'}|r|R_{n''\ell''}\rangle\langle Y_{\ell'm'_\ell}|\cos\theta|Y_{\ell''m''_\ell}\rangle\right|^2 \tag{2.65}$$

The radial part of the integral is evaluated numerically whereas the angular part has analytical solutions since $Y_{\ell m_\ell}$ are spherical harmonics (see exercise 2). The angular part is responsible for the selection rules

$$\Delta\ell = \ell' - \ell'' = \pm 1 \tag{2.66}$$

and

$$\Delta m = m' - m'' = 0 \tag{2.67}$$

in the case of *linearly* polarized light.

The parity (Laporte) selection rule

The parity operator $\hat{E}^*$ inverts the coordinates of all particles:

$$\hat{E}^*\,\Psi(x_1,\ldots,z_N) = \Psi(-x_1,\ldots,-z_N). \tag{2.68}$$

Because the kinetic and potential energy operators in the Hamiltonian only depend on the coordinates squared, the Hamiltonian commutes with the parity operator:

$$\left[\hat{E}^*, \hat{H}\right] = 0 \tag{2.69}$$

and therefore the eigenstates of the Hamiltonian are also eigenstates of the parity operator:

$$\hat{E}^*\,\Psi(x_1,\ldots,z_N) = \pm\,\Psi(x_1,\ldots,z_N). \tag{2.70}$$

States with eigenvalue $+1$ have **positive parity**, states with eigenvalue -1 have **negative parity**. The transition moment has negative parity:

$$\hat{E}^*\vec{\mu}(x,y,z) = \vec{\mu}(-x,-y,-z) = -\vec{\mu}(x,y,z). \tag{2.71}$$

Because the integral over a function of negative parity vanishes, dipole transitions are only allowed between states of opposite parity:

$$+ \leftrightarrow -, + \nleftrightarrow +, - \nleftrightarrow -. \tag{2.72}$$

The same argumentation can easily be extended to the derivation of magnetic-dipole or electric-quadrupole selection rules as well as selection rules for multiphoton processes.

2.2.2 Spectra of hydrogen and other one-electron atoms

The spectra of hydrogen and hydrogen-like atoms have been of importance for the development of quantum mechanics and for detecting and recognizing the significance of fine, hyperfine and quantum-electrodynamics effects. They are also the source of precious information on fundamental constants such as Rydberg's constant and the fine-structure constant. If fine, hyperfine, and quantum-electrodynamics effects are neglected, the energy level structure of the hydrogen atom is given by Equation (2.2) and is characterized by a high-degree of degeneracy. The allowed electronic transitions can be predicted using Equation (2.66) and their wavenumbers determined using Equation (2.73)

$$\tilde{\nu} = \frac{R_M}{n''^2} - \frac{R_M}{n'^2} \tag{2.73}$$

which, for $n'' = 2$, reduces to Balmer's formula. The transitions obeying the selection rule (2.66) are depicted schematically in Figure 2.4a, in which, for simplicity, only transitions from and to the $n = 1$ and $n = 2$ levels are indicated by double-headed arrows.

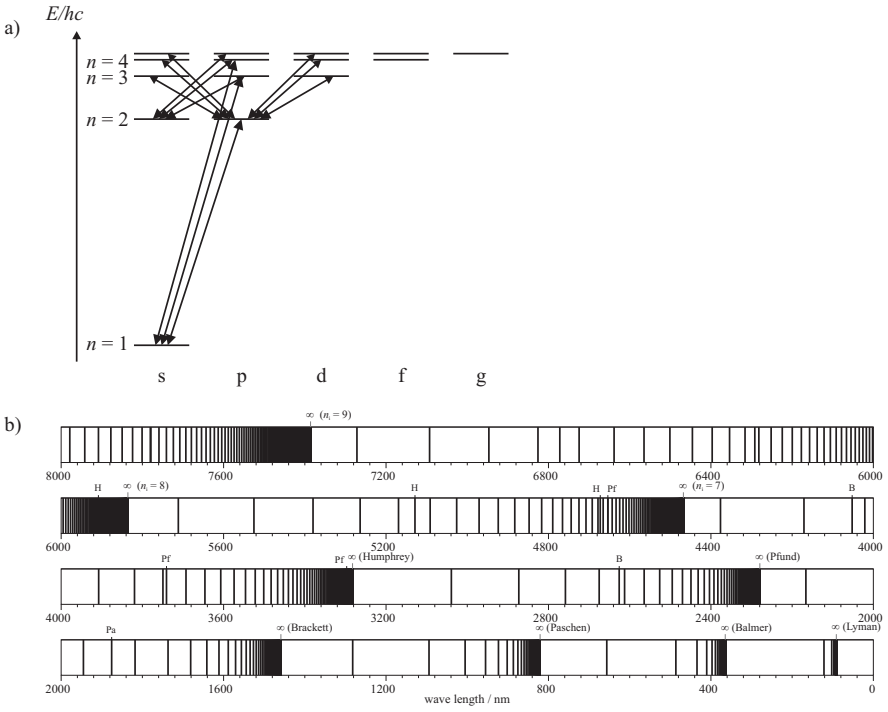

Figure 2.4: a) Energy level diagram of the H atom neglecting fine, hyperfine, and quantum electrodynamics effects. Possible single-photon transitions to and from the $n = 1$ and 2 levels are indicated by double-headed arrows. b) Schematic spectrum of H showing that the electronic spectrum extends from the microwave to the vacuum ultraviolet ranges of the electromagnetic spectrum.

Because of their importance, many transitions have been given individual names. Lines involving $n = 1$, 2, 3, 4, 5, and 6 as lower levels are called Lyman, Balmer, Paschen, Brackett, Pfund, and Humphrey lines, respectively. Above $n = 6$, one uses the n value of the lower level to label the transitions. Lines with $\Delta n = n' - n'' = 1, 2, 3, 4, 5, \ldots$ are labeled $\alpha, \beta, \gamma, \delta, \ldots$, respectively. Balmer β, for instance, designates the transition from $n = 2$ to $n = 4$. The spectral positions of the allowed transitions are indicated in the schematic spectrum presented in Figure 2.4b.

The fine and hyperfine structure of the $n = 1$ and $n = 2$ manifolds of the hydrogen atom are shown in Figure 2.5. The splitting of $\approx 0.0475\,\mathrm{cm}^{-1}$ of the 1s $^2\mathrm{S}_{1/2}$ ground state results from the hyperfine interaction. This splitting scales with n^{-3} and rapidly decreases with increasing n value, and also with increasing ℓ value. The spin-orbit splittings, which are zero for s levels, are largest for p levels and also scale as n^{-3}. The two components of the ^{2}P level with $J = 1/2$ and 3/2 are separated by $\approx 0.365\,\mathrm{cm}^{-1}$.

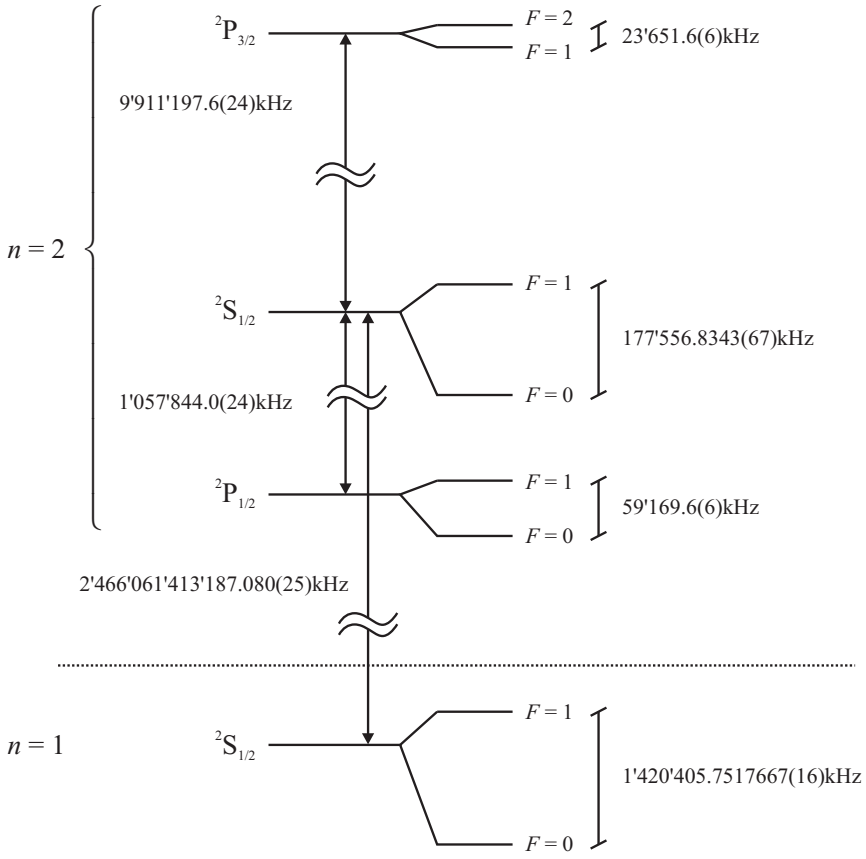

Figure 2.5: Fine and hyperfine structure of the $n = 1$ and $n = 2$ levels of the hydrogen atom.

High-resolution spectroscopy of hydrogen-like atoms such as H, He^+, Li^{2+}, Be^{3+}... and their isotopes continues to stimulate methodological and instrumental progress in electronic spectroscopy. Measurements on "artificial" hydrogen-like atoms such as positronium (atom consisting of an electron and a positron), protonium (atom consisting of a proton and an antiproton), antihydrogen (atom consisting of an antiproton and a positron), muonium (atom consisting of a positive muon μ^+ and an electron), antimuonium (atom consisting of a negative muon μ^- and a positron), etc., have the potential of providing new insights into fundamental physical laws and symmetries and their violations.

2.2.3 Spectra of alkali-metal atoms

A schematic energy level diagram showing the single-photon transitions that can be observed in the spectra of the alkali-metal atoms is presented in Figure 2.6. The ground-state configuration corresponds to a closed-shell rare-gas-atom configuration with a single valence n_0s electron with $n_0 = 2, 3, 4, 5$ and 6 for Li, Na, K, Rb and Cs, respectively. The energetic positions of these levels can be determined accurately from Equation (2.2). The Laporte selection rule (Equation (2.72)) restricts the observable single-photon transitions to those drawn as double-headed arrows in Figure 2.6. Neglecting the fine and hyperfine structures, their wave numbers can be determined using:

$$\tilde{\nu} = \frac{R_M}{(n'' - \delta_{\ell''})^2} - \frac{R_M}{(n' - \delta_{\ell'})^2}. \tag{2.74}$$

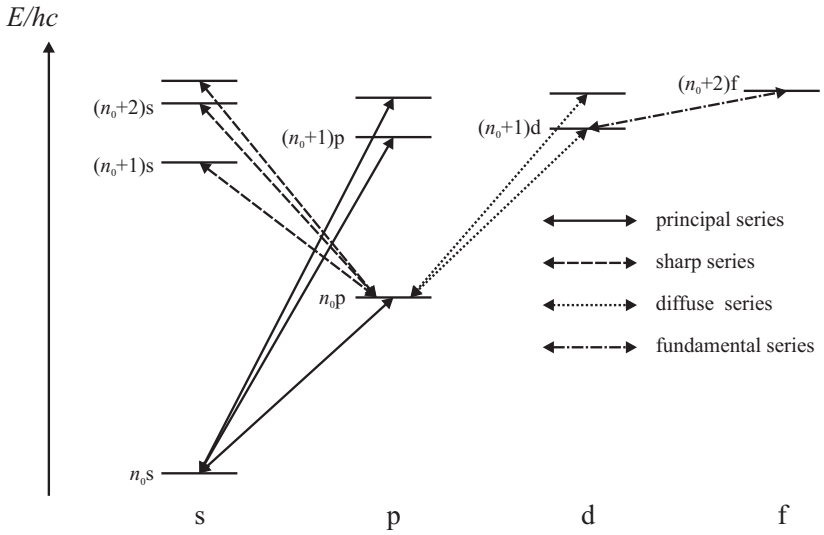

Figure 2.6: Schematic diagram showing the transitions that can be observed in the single-photon spectrum of the alkali-metal atoms.

The deviation from hydrogenic behavior is accounted for by the ℓ-dependent quantum defects. Transitions from (or to) the lowest energy levels can be grouped in Rydberg series, which have been called principal, sharp, diffuse and fundamental. Comparing Figure 2.6 with Figure 2.4, one can see that the principal series of the alkali metal atoms (called principal because it is observed in absorption and emission) corresponds to the Lyman lines of H, the diffuse and sharp series to the Balmer lines, and the fundamental series to the Paschen lines. The quantum defects are only very weakly dependent on the energy. Neglecting this dependence, the quantum defects of the sodium atom are $\delta_s \approx 1.35$, $\delta_p \approx 0.86$, $\delta_d \approx 0.014$, and $\delta_f \approx 0$, so that the lowest-frequency line of the principal series (called the sodium D line because it is a doublet, see below) lies in the yellow range of the electromagnetic spectrum, and not in the VUV as Lyman α. The fact that the n_0p $\leftarrow$ n_0s lines of the alkali metal atoms lie in the visible range of the electromagnetic spectrum makes them readily accessible with commercial laser sources, and therefore extensively studied and exploited in atomic-physics experiments.

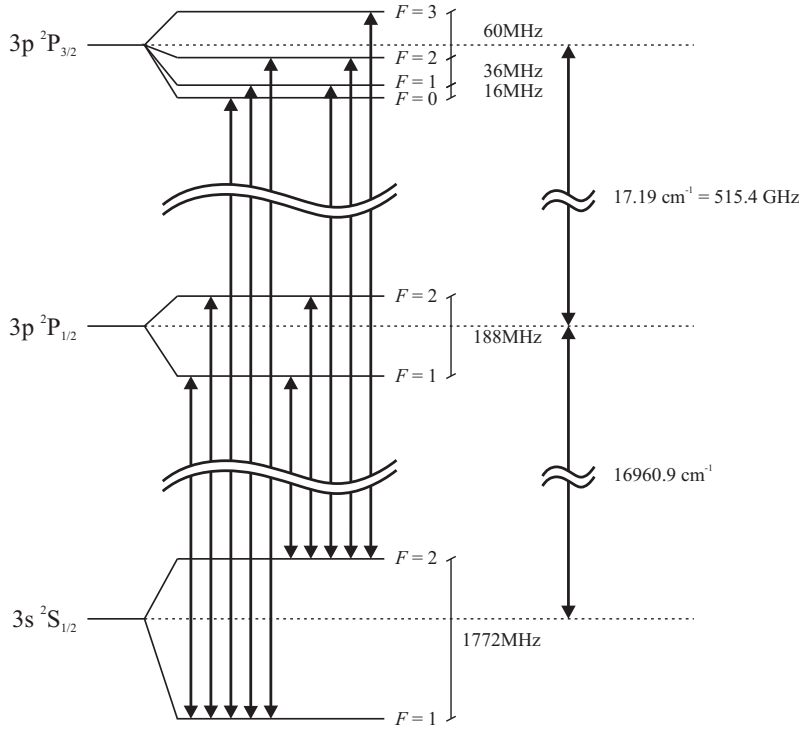

Figure 2.7: Schematic diagram showing the fine and hyperfine structure of the 3s and 3p levels involved in the lowest-frequency line of the principal series of ^{23}Na.

Most transitions of the alkali-metal atoms reveal fine and hyperfine structures. As in the case of H, the hyperfine-structure splittings are largest in the ground state (3s $^2S_{1/2}$ in the

case of Na) and the fine-structure splittings are largest in the lowest-lying p level (3p $^2\mathrm{P}_J$ with $J = 1/2, 3/2$ in the case of Na). The details of the structure of these two levels of Na are presented in Figure 2.7. At low resolution, the 3p←3s line appears as a doublet with two components at 16960.9 cm^{-1} and 16978.1 cm^{-1}, separated by an interval of 17.2 cm^{-1} corresponding to the spin-orbit splitting of the 3p state. The second largest splitting ($\approx 0.06\,\mathrm{cm}^{-1}$) in the spectrum arises from the hyperfine splitting of 1772 MHz of the 3s state. Finally, splittings of less than 200 MHz result from the hyperfine structure of the 3p levels.

2.2.4 Spectra of the rare gas atoms

The $^1\mathrm{S}_0$ ground state of the rare-gas atoms (Rg=Ne, Ar, Kr and Xe) results from the full-shell configurations ($[\ldots](n_0\mathrm{p})^6$ with $n_0 = 2, 3, 4$ and 5 for Ne, Ar, Kr, and Xe, respectively). Single-photon absorption by electrons in the $(n_0\mathrm{p})^6$ orbitals leads to the excitation of $J = 1$ states of the configurations $[\ldots](n_0\mathrm{p})^5(n\mathrm{s})^1$ and $[\ldots](n_0\mathrm{p})^5(n\mathrm{d})^1$.

Compared to H and the alkali-metal atoms discussed in the previous examples, the lowest excited electronic configurations contain two, instead of only one, unpaired electrons, which leads to both $S = 0$ and $S = 1$ states. Moreover, these states form Rydberg series that converge on two closely spaced ionization limits corresponding to the two spin-orbit components ($J^+ = 1/2, 3/2$) of the $^2\mathrm{P}_{J^+}$ ground state of Rg^+, rather than on a single ionization limit, as is the case for H and the alkali-metal atoms.

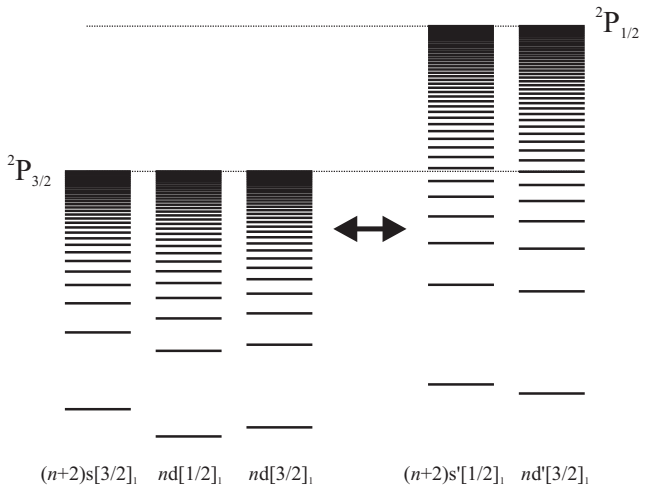

Figure 2.8: Schematic diagram showing Rydberg series converging to the two spin-orbit components $^2\mathrm{P}_J$ ($J = 1/2, 3/2$) of the rare gas atomic ions Rg^+. The series are designated in Racah's notation as $n\ell'[k]_J$, the prime designating series converging on the upper ($^2\mathrm{P}_{1/2}$) ionization threshold. Interaction between series are represented by horizontal arrows.

Figure 2.8 depicts schematically the $J = 1$ Rydberg series of the rare-gas atoms located below the $^2P_{J^+}$ ($J^+ = 1/2, 3/2$) ionization thresholds that are optically accessible from the $^1S_0$ ground state. Two angular momentum coupling schemes are used to label these Rydberg states. The first one corresponds to the familiar LS-coupling scheme discussed in Section 2.1.4 and tends to be realized, if at all, only for the lowest Rydberg states and the lightest atoms. Five series arise from the optically allowed p→s and p→d transitions, two s series ($(n_0p)^5(ns)^1$ $^3P_1$ and $^1P_1$) and three d series ($(n_0p)^5(nd)^1$ $^3D_1$, $^3P_1$ and $^1P_1$). The second one is a variant of the jj coupling scheme, and becomes an increasingly exact representation at high n values, when the spin-orbit coupling in the $^2P_{J^+}$ ion core becomes stronger than the electrostatic (including exchange) interaction between the Rydberg and the core electrons. As a result, the core and Rydberg electrons are decoupled, and J^+ becomes a good quantum number instead of S. In this labeling scheme, the states are designated $(^2P_{J^+})n\ell[k]_J$, k being the quantum number resulting from the addition of $\vec{J^+}$ and $\vec{\ell}$. The five optically accessible $J = 1$ series are labeled $ns[3/2]_1$, $ns'[1/2]_1$, $nd[1/2]_1$, $nd[3/2]_1$, $nd'[3/2]_1$, the "prime" being used to designate the two series converging to the $^2P_{1/2}$ ionization limit (see Figure 2.8).

Several sections of the single-photon VUV spectrum of Ar are presented in Figure 2.9. Figure 2.9a corresponds to the region where Rydberg states of principal quantum number $n \geq 33$ below the $^2P_{3/2}$ ionization limit can be excited from the ground state. In the region below 127060 cm^{-1}, only the $nd[3/2]_1$ and $ns[3/2]_1$ carry intensity. These two series are almost degenerate. The splittings can hardly be seen on the wave-number scale used to draw the spectrum, but are clearly visible on the expanded scale of the spectrum labeled B, which corresponds to the region of principal quantum number around $n = 55$. The high-n region of the spectrum is also displayed on an enlarged scale in the spectrum labeled C. The $nd[1/2]_1$ series is extremely weak at n values below 50, but becomes the dominant series beyond $n = 80$. In an unperturbed Rydberg series, the intensity should decrease as n^{-3}, as explained previously. The anomalous intensity distribution of the $nd[1/2]_1$ series has its origin in the interactions with the series converging to the $^2P_{1/2}$ ion core, which are such that, in some spectral regions, it has almost pure $S = 1$ character and cannot be excited from the $S = 0$ ground state. Figure 2.9b displays a section of the VUV spectrum of Ar in the region between the $^2P_{3/2}$ and $^2P_{1/2}$ ionization limits. The $ns'[1/2]_1$ and $nd'[3/2]_1$ series appear as sharp, symmetric, and broad, asymmetric autoionization resonances in this region, respectively.

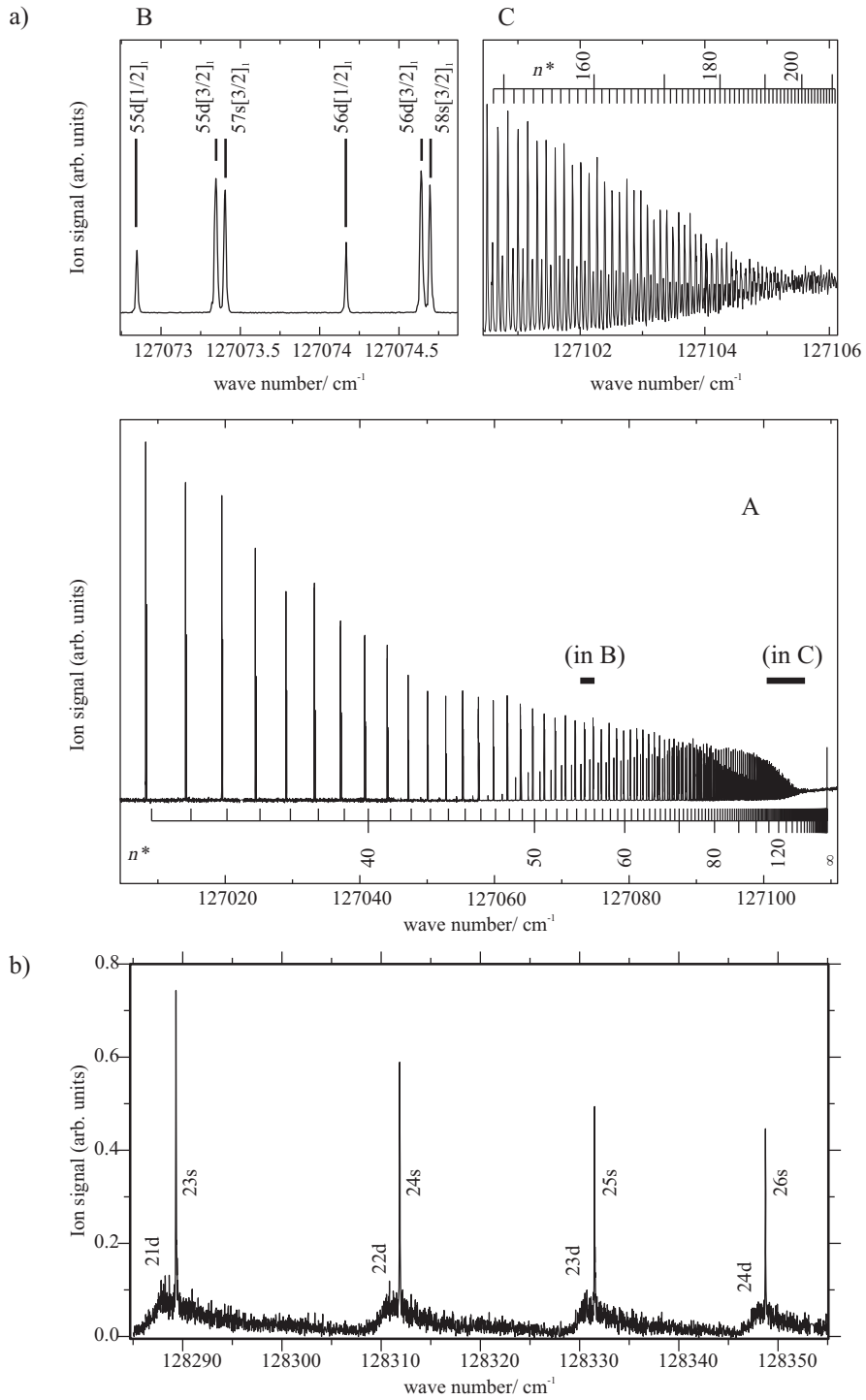

Figure 2.9: High-resolution VUV laser spectra of Ar recorded with a narrow-band laser. a) Region below the $^2P_{3/2}$ ionization threshold showing the perturbed $ns/d[k]_{J=1}$ series. The spectra shown labeled B and C represent sections of the spectrum labeled A presented on an enlarged scale. b) Region above the $^2P_{3/2}$ revealing the broad asymmetric $nd'[3/2]_1$, and the narrow, symmetric $ns'[1/2]_1$ resonances (adapted from U. Hollenstein, Diss. ETH Nr. 15237 (2003)).